Research Signpost
37/661 (2), Fort P.O.
Trivandrum-695 023
Kerala, India

Frontiers in Nanoscience for Biomedical Research, 2014: 00-000 ISBN: 978-81-308-0537-5
Editor: Kazushige Yokoyama

# 5. Bioimaging of cancer and inflammation with SapC-DOPS proteoliposomes

Víctor M. Blanco and Xiaoyang Qi
*Division of Hematology and Oncology, Department of Internal Medicine, University of Cincinnati College of Medicine, Cincinnati, Ohio, USA*

**Abstract.** Since their initial characterization and development about 30 years ago, nanovesicles have gained much relevance as vehicles to increase efficacy and specificity in the delivery of therapeutic agents. As research on nanocarriers expanded, in the last few years there have been several studies showing, in cell culture-based assays and in preclinical models of human illnesses, the feasibility and practicality of using lipid- or polymer-based nanovesicles as imaging agents. In this chapter we review these recent approaches, focusing on the different strategies employed to achieve selective or specific labeling of target cells and tissues, and summarize the advantages and pitfalls of different molecular markers used to visualize them. We also describe our own experience using saposin C (SapC) coupled dioleoylphosphatidylserine (DOPS) nanovesicles. By taking advantage of the affinity of SapC-DOPS complexes for surface exposed phosphatidylserine molecules on the cell membrane, characteristic of many cancer and inflammatory cells, we tested the ability of SapC-DOPS, labeled with a far-red fluorescent probe or superparamagnetic iron oxide beads, to visualize non-apoptotic tumors and inflammatory conditions *in vivo*. Our experiments

Correspondence/Reprint request: Dr. Xiaoyang Qi, Division of Hematology and Oncology, Department of Internal Medicine, University of Cincinnati College of Medicine, Cincinnati, Ohio, USA. E-mail: xiaoyang.qi@uc.edu

showed that SapC-DOPS nanovesicles are robust and effective tools for the bioimaging of cancer and inflammation, and might be useful to aid in the diagnosis of other physiopathological conditions as well.

## Introduction

Biomedical imaging modalities such as magnetic resonance (MR), nuclear medicine (e.g. PET), computed tomography and ultrasound are irreplaceable tools in the detection and management of lesions and pathological conditions [1-4]. Each technique has its strengths and limitations, and accurate diagnosis, prognosis and treatment usually requires a combined, multimodal approach involving two or more of these techniques; this approach is however expensive and not always feasible to implement. Whereas the introduction of novel contrast agents has improved the sensitivity and spatial/temporal resolution of these traditional imaging modalities and has helped reduce their limitations, advances in photonics and digital sensor technologies have in turn made optical imaging a powerful tool to capture phyisiopatological events with cellular and subcellular (molecular) resolution [5]. Much effort is now being devoted to design more stable, more efficient and less toxic imaging compounds, and new or more sophisticated nanostructures that can carry them to target tissues and cells. As researchers continue to characterize the molecular profile of physiopathological processes such as inflammation and infection, and diseases like autoimmune disorders and cancer, there are strong incentives to find target-specific biomarkers to guide the delivery of imaging probes, contrast agents and therapeutics. Particular interest is centered in creating multimodal and multifunctional nanoprobes and devices, to combine therapeutic and diagnostic (theranostic) capabilities [6,7]. An exciting development resulting from this deeper understanding are the newer "smart", activatable compounds and nanoprobes, that exploit distinctive features of the tumor microenvironment, such as an increased acidity, or the enhanced activity of cellular proteases, to selectively release and/or activate imaging probes or therapeutic drugs [8-11]. With these advances, we are witnessing the rise of a new generation of more sensitive and specific probes that yield information not only on the size, location, and vascular pattern of tumors, but also on the functional status of the disease [12].

## Platforms for nanocarriers

Liposome and polymer-protein nanocarriers were first developed as vehicles to improve the pharmacokinetic properties of chemotherapy drugs and to deliver water-insoluble drugs to tumor cells, either passively, by

relying on the enhanced permeability and retention (EPR) effect and impaired lymphatic drainage characteristic of "leaky" tumor vasculature, or actively, by incorporating ligands recognized selectively by tumor cells [13,14]. The use of nanocarriers has since been extended to imaging modalities like MRI, ultrasound and optical imaging techniques, to increase the payload and hence the sensitivity of contrast agents like $Gd^{3+}$, iron oxide crystals, and fluorescent probes. Although most of these developments are still in preclinical stages, their translation to the clinical setting is being aided by steady advances in imaging technology and the rapidly growing field of nanomaterial sciences [15].

The rationale behind the design of nanoparticles for bioimaging should contemplate the following considerations: i) biocompatibility: the agent must have minimal or negligible toxicity; also, it must be biodegradable and/or excretable, ii) specificity: it must accumulate and be selectively retained in target sites, in order to achieve an adequate target-to-background ratio of the images, and iii) sensitivity: it must generate a signal strong enough as to be clearly detected by the imaging modality used to identify it. Effective carriers must also be able to carry large payloads, be functionalized with target-specific ligands or moieties, and avoid early interaction with homeostatic defense mechanisms (e.g. immune surveillance). The latter problem is commonly attenuated by coating the nanoparticles with inert polymers such as polyethylene glycol (PEG) or dextran [16,17].

The variety of nanomaterials employed for molecular imaging has grown enormously in the last decade and continues to expand [18,19]. What follows is a brief description of the ones that are most commonly used.

**Metal oxides.** These include microcrystalline superparamagnetic iron oxide (SPIO; 50-150 nm) and ultrasmall superparamagnetic iron oxide (USPIO; <50 nm) nanoparticles, coated with a stabilizing, biocompatible and hydrophilic polymer, typically dextran. Unlike paramagnetic contrast agents such as metal chelates (e.g. Gd-DTPA), which produce positive signal enhancement of MR images, iron (U)SPIOs produce a localized decrease in signal (negative enhancement) in T2 weighted MR images. Compared with $Gd_3$-chelates, (U)SPIOs produce stronger MR relaxation, have much lower toxicity, and can be fine-tuned for specific applications. These particles can be dispersed in organic solvents and aqueous solutions and loaded within liposomes (magnetoliposomes), micelles, polymer-shell nanospheres, etc. [20,21], to increase the MRI signal contrast and to confer target specificity.

**Polymers.** Biocompatible, polymeric nanoparticles of 10-1000 nm in size constitute flexible tools for bioimaging and drug delivery [22]. These

structures, made from synthetic polymers such as poly-lactic acid, or from natural polymers such as chitosan, include dendrimers and multivalent, branched, graft, and block polymers [23,24]. They are suitable carriers for encapsulated or attached drugs and imaging probes, possess prolonged plasma half-lives, are highly stable, and are biologically inert.

**Quantum dots.** Quantum dots (QDs) are semiconductor, fluorescence-emitting nanocrystals with cores typically composed of cadmium selenide, lead selenide, or indium arsenide coated with a semiconductor shell and a polymer, which enables the linkage of proteins, small molecules, etc. Advantages of QDs over organic fluorescent dyes in bioimaging applications relate to their higher fluorescent quantum yield, size and composition dependent (tunable) fluorescence, photochemical stability, resistance to photobleaching and potential for multifunctionalization. The main disadvantage of QDs resides in their potential toxicity and apparent long-term retention (impaired clearance) in the body [25,26].

**Lipid-based nanovesicles.** Lipid-based nanovesicles are derived from self-assembling, colloidal aggregates of amphiphilic lipids, (e.g. phospholipids, glycolipids, and aminolipids) and include liposomes, micelles and microemulsions [27,28]. The amphiphilic nature of these structures imparts them with valuable functional properties: hydrophilic cargos can be enclosed in their aqueous lumen, hydrophobic compounds can be carried in their hydrophobic domains, and their surfaces can be functionalized by incorporating target-specific ligands such as peptides and antibodies. Other advantages of lipidic nanovesicles over other nanocarriers reside in their simpler synthesis, high biocompatibility, low toxicity and large payload capacity. Drawbacks include uptake by phagocytic cells of the reticuloendothelial system (RES), poor mechanical stability which can lead to leakage or rupture of the vesicles. These problems can be reduced by coating them with inert, neutral coatings such as PEG [16].

## Targeting strategies

Most of the nanoparticles currently used for cancer and inflammation imaging and/or drug delivery rely on their passive accumulation in the target tissue, determined by the greater permeability typical of the vasculature of solid tumors and inflammatory processes (EPR effect) [29,30]. In addition, since most nanoparticles are eventually phagocytosed by cells such as macrophages, inflammatory cell infiltrates are frequently assessed with untargeted magnetic particles using MRI [31-33]. Targeted

approaches are more difficult, but more efficient than passive ones. Complete reliance on the EPR effect precludes early tumor detection and the identification of micrometastases, and bears an increased risk of toxicity due to the prolonged retention of nanoparticles in the body. Clinical data also suggests that its efficacy is at best modest, with a just a small fraction of the administered dose reaching the intended target, and most of it localizing to the RES (spleen, liver, bone marrow) and to first-pass organs such as kidneys and lungs [15,34,35]. A great deal of effort is therefore being devoted to design systems with disease-specific targeting capacity. The latter is conferred by peptides, proteins (generally antibodies or antibody fragments), nucleic acids (aptamers), vitamins, etc. that target membrane carbohydrates, receptors, and antigens overexpressed in cancer cells, determining the internalization of the carrier into the tumor cell and the subsequent release of the drug or imaging agent [36,37]. Nevertheless, it is noteworthy that although targeted strategies indeed result in increased tumor signal, most still depend primarily on passive accumulation mechanisms due to the EPR effect [38]. Below we present relevant examples of targeted strategies for tumor and inflammation imaging that proved to be effective in preclinical (animal) models.

**Membrane receptors.** The epidermal growth factor receptor variant III (EGFRvIII) is a tumor-specific mutation widely expressed in glioblastoma cells. A polyclonal rabbit antibody raised against EGFRvIII and conjugated to triblock copolymer-coated iron oxide nanoparticles (EGFRvIIIAb-IONPs) has been developed as a theranostic (diagnostic and therapeutic) contrast agent for MRI. Upon delivery of EGFRvIIIAb-IONPs by convection enhanced delivery, both effective tumor uptake and increased survival rate in human GBM mouse model were observed [39].

Overexpression of c-Met, the receptor for hepatocyte growth factor, has been implicated in the progression of non-small cell lung and other human cancers. An anti-c-Met single chain variable fragment (scFv) antibody was conjugated to doxorubicin-containing liposomes and quantum dots for *in vivo* drug delivery and fluorescent imaging, respectively, in a SCID mouse xenograft model bearing a human large-cell lung tumor (H460) [40].

The identification of circulating tumor cells (CTCs) from patients' blood is a long-sought goal that would allow detection of metastatic tumor cells and aid in the design of personalized therapies. Using surface-enhanced Raman spectroscopy, gold nanoparticles linked to an EGF peptide and coated with thiolated PEG (to avoid interaction with blood cells and prevent aggregation) were used to detect CTCs in the peripheral blood of patients with squamous cell carcinoma of the head and neck [41].

Folic acid receptors (FRs) are mostly restricted to tubular cells in the kidneys, but are overexpressed in about 40% of human cancers, and also in activated macrophages [42]; the targeting of FRs is thus an enticing goal for the diagnosis and therapy of cancer and inflammation. The successful implementation of folate-targeted radionuclides for the clinical diagnosis of diseases such as ovarian cancer and arthritis, and the use folate-fluorescent dye complexes for endoscopic detection and surgical removal of mucosal malignancies prompted the development of folate-targeted nanoparticles [43,44]. These include ferromagnetic particles, tested in xenografted nasopharyngeal epidermal carcinoma cells [45], hybrid micelle-encapsulated USPIOs used to visualize hepatoma xenografts [46], and self-assembling folate-heparin nanovesicles containing a NIRF dye for *in vivo* tumor visualization and photothermal ablation in mice bearing human breast adenocarcinoma (MCF-7) xenografts [47].

The transferrin receptor, crucial in maintaining cellular iron homeostasis, is highly expressed in many cancer cells. Transferrin-bound USPIO nanoparticles were first used to enhance MRI signal in rat mammary carcinoma [48]. Very recently, transferrin-conjugated PEGylated liposomes containing a NIR dye and an interferon-γ inducible protein-10 plasmid DNA were used for combined imaging and gene transfer both *in vitro* and *in vivo*, in a mouse breast cancer model [49]

Among several other cancer membrane receptors and proteins targeted by nanoparticulate systems in experimental models to date are the urokinase-type plasminogen activator receptor, detected in mammary tumors using MRI, [50] and the CD44 antigen, targeted with immunoliposomes designed for combined *in vivo* imaging/therapy in a mouse model of hepatocellular carcinoma [51].

**Adhesion molecules.** Integrins are adhesion molecules that are highly expressed in the neovasculature of actively growing tumors, and hence represent attractive targets for tumor-directed delivery of drugs and imaging agents [52]. Peptides with the arginine-glycine-aspartate (RGD) sequence mimic the natural ligands of the integrins αvβ3 and αvβ5and have been used for such purposes in several studies [53]. Prompted by the success of RGD-radionuclides or RGD-near-infrared fluorescent (NIRF) probes conjugates, amine-modified quantum dots (QD705) with attached RGD peptides were used for near-infrared imaging of tumor vasculature in U87MG human glioblastoma xenografts in mice [54]. More recently, a cyclic RGD peptide attached to liposomes was used for drug delivery and far-red fluorescent imaging (BODIPY fluorophore) of a metastatic pancreatic carcinoma mouse model [55].

**Activated endothelium.** The differential expression of proteins such as selectins and vascular cell adhesion molecule-1 (VCAM-1) by inflamed endothelium has been exploited to design probes for inflammation imaging [56]. For instance, echogenic immunoliposomes conjugated with either anti-VCAM, anti-intracellular adhesion molecule (ICAM), anti-tissue factor, anti-fibrin, and anti-fibrinogen were employed for intravascular ultrasonic detection of atheroma components in swine [57]. The use of magneto-optical nanoparticles functionalized with anti-VCAM antibodies for dual MR/intravital fluorescence microscopy was first reported in a model of focal ear inflammation in mice [58]. Further work using anti-VCAM-1 antibodies or targeting peptides showed the feasibility of imaging atherosclerotic plaques [59] or renal inflammation [60] by MRI in hyperlipidemic mice fed a high-fat diet. Larger (1 um) iron oxide microparticles coupled to an anti-VCAM-1 antibody were also used for endovascular imaging of acute brain inflammation [61]. Magnetic nanoparticles coupled to anti-selectin antibodies or to selectin-binding molecules were also effective for MRI in rodent models of focal ear inflammation [62], traumatic brain injury [63], multiple sclerosis [64], stroke [65] and aortic aneurysm [66].

**Inflammatory cells.** An alternative and complementary approach to visualize focal or systemic inflammation and autoimmune disease resides in the identification of resident or circulating immune cells. As mentioned before, the unspecific phagocytosis of nanoparticles by activated immune cells has been widely exploited for inflammation imaging [67]. Targeted approaches are exemplified by the use of iron oxide nanospheres linked to a major histocompatibility complex ligand peptide and labeled with fluorescein, to demonstrate the accumulation of autoreactive diabetogenic CD8+ T cells in the pancreas of diabetic mice [68], and of polymeric dextran nanoparticles with multimodal (PET, MRI and optical) imaging capabilities to image macrophages in atherosclerotic lesions in mice [69].

**Phosphatidylserine.** Phosphatidylserine, a negatively charged membrane phospholipid that is preferentially exposed in the outer membranes of apoptotic cells and also in many tumor and tumor-associated vascular cells, constitutes an attractive pan-tumoral and pan-inflammatory cell marker [70-74]. A number of peptides and proteins that bind phosphatidylserine have been explored for the detection of apoptosis *in vivo* [75,76]. The one most studied is the endogenous protein annexin A5, which has been labeled to radionuclides,conjugated to NIRF dyes, or coupled to ferromagnetic particles to estimate the extent of tumor apoptosis following chemo- or radiotherapy in animal models and humans [77,78]. Annexin A5-coupled QDs loaded with

Gd-DTPA have been also tested for dual imaging of apoptosis and activated platelets using MR and optical techniques [79]. More recently, two papers described multimodal imaging of apoptosis in atherosclerosis, using Annexin A5-conjugated, $Gd_3$-labeled lipidic micelles containing a NIR dye [80] and in inflammatory and cancer disease models, using 111In-labeled, annexin A5-conjugated polymeric micelles [81].

In the following sections we present a summary of our research using phosphatidylserine -binding lipid-protein nanovesicles (SapC-DOPS) for *in vivo* MRI and optical imaging of cancer cells and inflammatory processes.

## SapC-DOPS nanovesicles as bimodal agents for the detection of cancer and inflammatory processes

SapC and DOPS are two naturally-occurring molecules present in animal cells. SapC is a small, heat-stable, fusogenic protein that activates glucosylceramidase (glucocerebrosidase), a lysosomal enzyme that catalyzes the breakdown of glucosylceramide into glucose and ceramide [82,83]. Binding of SapC to phosphatidylserine is required for activation of glucosylceramidase. When combined in aqueous solution at acidic pH, Saposin-C and DOPS readily assemble into proteoliposomes (SapC-DOPS) with a mean diameter of ~200 nm [84-86]. Accordingly, our studies demonstrated that SapC-DOPS vesicles have preferential affinity for phosphatidylserine -enriched membrane domains, which have been shown to be common in many types of tumor cells and tumor-associated endothelial cells [70-72], and also in apoptotic cells and activated immune cells characteristic of inflammatory foci [73,74]. We further documented the selective targeting and cytotoxic activity of SapC-DOPS towards a variety of human cancer cells, purportedly via activation of the ceramide- and caspase mediated apoptotic pathway [84,85]. In view of such properties, we explored the suitability of SapC-DOPS liposomes as vehicles to deliver an MRI contrast agent, i.e. ultrasmall superparamagnetic iron oxide (USPIO; ferumoxtran-10; Advanced Magnetics, Lexicon, MA), and the fluorescent probe CellVue Maroon (CVM; Molecular Targeting Technologies Inc., West Chester, PA) to tumor cells and inflammatory processes *in vivo*. Below we summarize these results, which show that SapC-DOPS liposomes are flexible, promising tools for the detection of tumors and inflammatory conditions *in vivo*.

**USPIO conjugation for tumor imaging with MR.** The encapsulation of USPIO (size ~20 nm) was achieved by adapting a chemical binding method described by Bogdanov et al. [87] as described in detail by Kaimal et al. [88] (Fig. 1A). We reported the ability of USPIO-conjugated SapC–DOPS

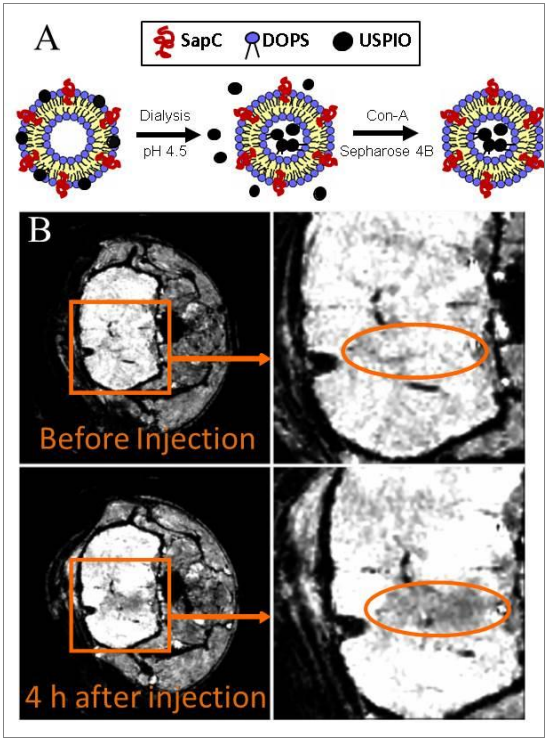


**Figure 1. SapC-DOPS-IO nanovesicles applied to MRI imaging. A)** Schematic diagram showing the last steps in the preparation of SapC-DOPS-IOs. After vesicle sizing using a 200-nm polycarbonate membrane, the vesicle suspension is dialyzed against a low pH (4.5) solution of NaCl and Na-citrate to remove USPIO particles attached to the vesicles' outer surfaces. Unencapsulated USPIOs are removed by gel filtration using a Con-A Sepharose 4B column. The nanovesicles are then stabilized by adding HEPES buffered to pH 8.0 (20 mM final HEPES concentration). **B)** High-resolution MRI of a glioma in a nude mouse *in vivo*. MRI was performed at 7 T. T2* weighted 3D FLASH sequence (TE/TR=10ms/20ms/FA=10°) were used with a 320×320×64 matrix and 3.2×3.2×0.64 cm FOV resulting in an isotropic 100 µm resolution. Imaging time: 16 min. 4 hours after intravenous injection of SapC–DOPS–IO (250 µl containing approx. 22 µg iron) negative contrast enhancement is observed.

nanovesicles (SapC–DOPS–IO) to detect neuroblastoma cells *in vitro* and *in vivo* using inductively coupled plasma-atomic emission spectroscopy (ICP-AES) and MRI [89]. We also tested SapC-DOPS-IOs' potential for visualizing brain tumors in mice. Fig. 1B shows T2* weighted MR images of

a mouse glioma before and after injection with SapC–DOPS–IO. The negative contrast enhancement observed in the lower image denotes effective targeting of the tumor by SapC–DOPS–IO (unpublished results).

**CVM conjugation for tumor and inflammation imaging.** We evaluated the feasibility of using SapC-DOPS nanovesicles to detect tumors and inflammatory foci using optical imaging in several animal models. The dye of choice was CVM, a far-red lipophilic compound (Ex max =647 nm; Em max = 667 nm). Imaging in the far red/near-infrared spectrum (600–1000 nm range) is currently the most effective and sensitive way to visualize small fluorescent probes *in vivo*, due to the increased penetration, decreased scattering and reduced absorbance of light in this wavelength range [89]. In addition, tissue auto-fluorescence is also greatly diminished in the near-infrared domain [19]. The IVIS (PerkinElmer) single-view 3D optical imaging system was used to perform *in vivo* detection of CVM (Ex=640; Em=700), with acquisition times ranging from 0.1 to 1 sec.

**Tumor imaging with *SapC-DOPS-CVM*.** We have reported the selective targeting of various cancer cells by SapC-DOPS *in vitro* [84,85]. This selectivity was further explored through co-cultures of normal (Schwann cells or brain astrocytes) and tumoral (SH-SY-5Y neuroblastoma or Gli36 glioma) human cells, which resemble more closely the cellular diversity found in tumors *in vivo*. Fig. 2 (A-B) shows microphotographs of these co-cultures after brief (30 min) exposure to SapC-DOPS-CVM. Schwann cells and astrocytes were labeled with the lipophilic dye PKH67, to distinguish them from their tumoral counterparts. It can be seen that the CVM fluorescence is located preferentially in tumor, rather than normal, cells. This correlates with the greater exposure of cell surface phosphatidylserine in the tumor cells, as assessed with Annexin A5 stain using flow cytometry (Fig. 2C).

The potential of SapC-DOPS-CVM nanovesicles for *in vivo* visualization of a variety of animal tumor models was assessed using the IVIS imaging system. Tumor cells expressed luciferase and tumor growth was monitored through luminescence. SapC-DOPS-CVM was injected intravenously and CVM fluorescence was assessed after 4-24 hs. Figure 2 shows pictures of SapC-DOPS-CVM signal localized to breast cancer (D), brain metastatic tumor (E), and glioblastoma (F). Fig. 2G shows confocal images of brain sections from glioblastoma-bearing mice showing tumor-specific SapC-DOPS-CVM uptake (red; upper panel) and minimal signal (lower panel) in a tumor-bearing mouse injected with DOPS-CVM. SapC-DOPS-CVM targeting of colon polyps in a colorectal cancer mouse model is shown in Fig. 2H. Fig. 2 (I-K) shows photographs of experimental lung tumors in mice

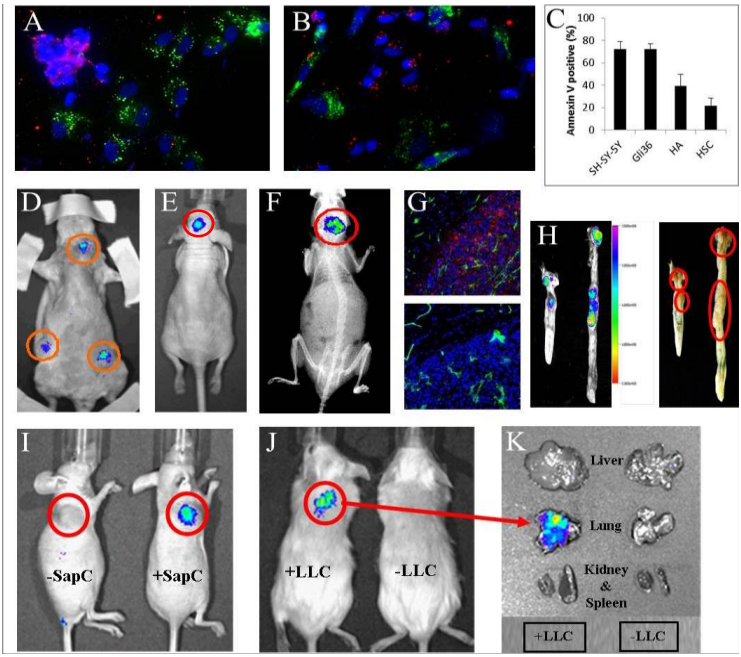


**Figure 2. Tumor targeting with SapC-DOPS-CVM. A)** Co-cultured human Schwann cells and SH-SY-5Y neuroblastoma cells. **B)** Co-cultured human astrocytes and Gli36 glioma cells. Schwann cells and astrocytes were pre-labeled with PKH67 (green). The co-cultures were treated with SapC-DOPS-CVM (30 min), fixed and mounted in aqueous mounting medium containing DAPI, to visualize nuclei (blue). Note the preferential uptake of SapC-DOPS-CVM by cancer cells. **C)** Membrane PS levels in the cell types shown in A and B, as assessed with a fluorometric annexin A5 assay. Higher PS levels in tumor cells correlate with increased SapC-DOPS-CVM uptake. **D)** *In vivo* imaging of SapC-DOPS-CVM fluorescence in a rat model of breast cancer. **E)** *In vivo* imaging of SapC-DOPS-CVM fluorescence in a mouse model metastatic brain tumor, induced by intracarotid injection of luciferase-expressing, human breast cancer, MDA-MB-231 cells). **F)** SapC-DOPS-CVM targeting of brain tumor . Superimposed X-ray and fluorescence images of a nude female mouse bearing a glioblastoma induced by intracranial injection of human U87-ΔEGFR-Luc cells. **G)** Brain sections from mice like the one depicted in (F) reveal selective uptake of SapC-DOPS-CVM (top) but not DOPS-CVM (bottom) by tumor cells. Green signal denotes blood vessels stained with lectin-FITC. **H)** *Ex-vivo* visualization of colon polyps in a mouse colorectal cancer model, targeted with SapC-DOPS-CVM. **I-K)** Lung tumors visualized *in vivo* with SapC-DOPS-CVM. **I)** Nude mice bearing subcutaneous LLC cell xenografts and injected with DOPS-CVM (left) or SapC-DOPS-CVM (right) **J)** SapC-DOPS-CVM targeting of lung cancer (LLC+) induced by intravenous injection

**Figure 2.** Legend continued

of LLC cells in a FVB mouse. **K)** *Ex-vivo* fluorescence images of dissected organs from the LLC- tumor-bearing mouse and the control (LLC-) mouse showing specific SapC-DOPS-CVM targeting of the diseased lung.

induced via subcutaneous xenograft (I) or intravenous injection (J) of Lewis lung carcinoma (LLC) cells. Excised organs form the animals shown in (J) are shown in (K).

**Inflammatory disease imaging with SapC-DOPS-CVM.** Increased cell membrane phosphatidylserine externalization is a common feature of the tissue damage and extensive apoptosis of immune cells that occur in inflammatory conditions [73,74]. In light of this, we reasoned that SapC-DOPS nanovesiclescould be useful in the detection of inflammatory diseases. We recently reported the use of SapC-DOPS for *in vivo* bioimaging of inflammatory arthritis in mice [90], demonstrating that the main target of SapC-DOPS in inflamed arthritic joints were neutrophils, which are known to externalize phosphatidylserine upon activation. We also conducted initial experiments to assess the ability of SapC-DOPS to target inflammation in DSS (dextran sulfate sodium)-induced murine colitis, an experimental model of human inflammatory bowel disease (IBD). Fig. 3 shows mice with and without DSS-induced colitis after injection with SapC-DOPS-CVM. CVM signal was detected only in the diseased colon, reinforcing the ability of SapC-DOPS to target inflamed tissues in preclinical models of inflammatory diseases.

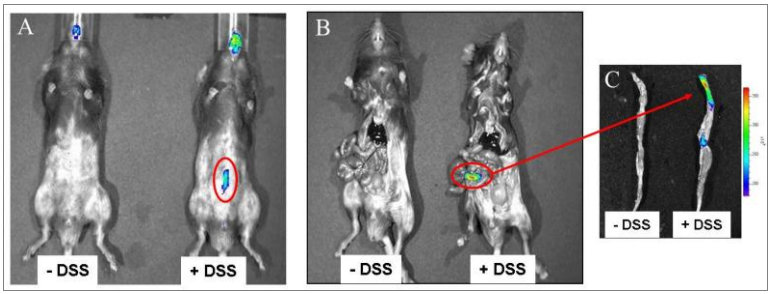


**Figure 3. SapC-DOPS-CVM targets inflamed colon in DSS-induced colitis in mice.** Wild-type PCTFlox (N) mice were dosed with 1.5% DSS in an acidified drinking water for 7 days. CVM fluorescent signal was determined 18 h after injection of SapC-DOPS-CVM. **A)** *In vivo* SapC-DOPS-CVM signal in mice without (-DSS) and with (DDS+) DDS-induced colitis. **B)** Exposed colons showing SapC-DOPS-CVM fluorescence only in the DDS+ mouse. **C)** *Ex-vivo* SapC-DOPS-CVM signal in excised colons.

## Seeing the forest for the trees: Targeting phosphatidylserine for the diagnosis and treatment of human disease

Paralleling the steady advances in nanotechnology, the field of biological imaging has experienced a dramatic growth in the last decade. A wide array of nanostructures with multifunctional capabilities is yielding promising results in basic research laboratories, and with them we are witnessing the advent of disease-specific therapeutics and personalized medicine. Although the number of nanocarrier-based diagnostic and therapeutic formulations approved for clinical use is, as compared with that of small molecules, still very small, a main advantage of nanoscale carriers over small molecules for imaging and therapy lies in the nanocarriers' large surface to volume ratio, which allows the attachment, embedding or encapsulation of several ligands with diagnostic or therapeutic properties. Another important benefit of such systems is that by combining materials with different biophysical properties, a more precise control of the timing and dosage of delivery of the imaging probe or drug is potentially achievable. Compared with other malignancies, the diagnosis and treatment of neoplasms often pose significant challenges because of the great heterogeneity of cancer cells. Although the repertoire of cancer biomarkers, mono- and macromolecular carriers and imaging probes continue to grow, practical limitations make it highly desirable to rely on approaches with broad applicability.

SapC-DOPS nanovesicles present a number of attractive features for the detection of conditions, such as cancer and inflammation, characterized by increased exposure of phosphatidylserine in the surface of cells. As our data show, they are broadly applicable to visualize multiple types of tumors and inflammatory conditions in animal models *in vivo*, making them a potentially useful pan-tumoral and pan-inflammatory diagnostic agent. SapC and DOPS are naturally-occuring molecules found in most human cells, and as such are highly biocompatible; as reported, supra-therapeutic doses had no acute or chronic toxicity, and no histopathological findings were observed in animal models [84]. As with most nanoparticles, they are subject however to uptake by phagocytic cells in the liver and spleen. We reported that clearance from these organs after intravenous SapC-DOPS injection takes about 48 hs in mice. Also, the bioavailability of SapC-DOPS is high, as denoted by the time-dependent accumulation of SapC-DOPS-CVM in an orthotopic glioblastoma mouse model (unpublished data). SapC-DOPS nanovesicles are also flexible platforms. As shown above, multimodal imaging is possible by encapsulation of magnetic nanoparticles and incorporation of fluorescent dyes for detection using MRI and optical imaging techniques [88,90]. Similarly, these nanovesicles can also be functionalized with different ligands

and moieties, to alter targeting specificity and/or to effect cytotoxicity in different ways. Thus, we believe that the demonstrated pro-apoptotic capacity of SapC-DOPS, combined with the imaging capabilities described and illustrated above, make these nanovesicles good candidates for theranostic applications in the clinical practice.

## Acknowledgments

We thank Dr. N.M. Brown and K. Setchell for the rat breast tumor model, Dr. J.S. Palumbo for the murine colitis model, Drs. T. Noah and N. Shroyer for the murine colon tumor model, and K. LaSance and Dr. L.C. Lemen for brain tumor imaging. This work was supported in part by University of Cincinnati Start Up fund (to Qi), NIH/NCI Grants Number 1R01CA158372-01 (to Qi), and New Drug State Key Project Grant Number 009ZX09102-205 (to Qi).

## References

1. Jaffer, F.A. and Weissleder, R. 2005, JAMA, 293, 855.
2. Faas, L. 2008, Mol. Oncol., 2, 115.
3. Kaimal, V., Leopold, W.R., and McConville, P. 2011, Tumor Models in Cancer Research, (Cancer Drug Discovery and Development). B.A. Teicher (Ed.), Springer Science+Business Media, 215
4. Yuan, B., and Rychak, J. 2013, Am. J. Pathol., 182, 305.
5. Taruttis A, Ntziachristos, V. 2012, AJR Am. J. Roentgenol., 99, 263.
6. Eifler, A.C., and Thaxton, C.S. 2011, Methods in Molecular Biology, 726, 325.
7. Cheng, Z., Al Zaki, A., Hui, J.Z., Muzykantov, V.R., and Tsourkas, A. 2012. Science, 338, 9030.
8. Danhier, F., Feron, O., and Préat, V. 2010, J. Control. Release, 148, 135–146.
9. Schellenberger, E. 2010, J. R. Soc. Interface, 6, Suppl 1, S83.
10. Swami, A., Shi, J, Gadde, S. Votruba, A.R., Kolishetti, N. and Farokhzad, O.C., 2012, Multifunctional Nanoparticles for Drug Delivery Applications: Imaging, Targeting, and Delivery, Nanostructure Science and Technology., S. Svenson and R.K. Prud'homme (Eds.), Springer Science+Business Media, 9.
11. MacEwan, S.R., and Chilkoti, A. 2013, WIREs Nanomed. Nanobiotechnol., 5: 31-48.
12. Michalski, M.H., and Chen, X. 2011, Eur. J. Nucl. Med. Mol. Imaging 38, 358.
13. Bangham, AD. 1993, Chem. Phys. Lipids, 64, 275.
14. Peer, D., Karp, J.M., Hong, S., Farokhzad, O., Margalit, R., and Langer, R. 2007, Nature Nanotechnology, 2, 751.
15. Choi, H.S. and John V. Frangioni 2010, Nanoparticles for biomedical imaging: fundamentals of clinical translation. Mol Imaging . 9(6): 291–310
16. Oku, N., Namba, Y., and Okada, S. 1992, Biochim. Biophys. Acta, 1126, 255.

17. Yu, M, Huang, S., Yu K.J., and Morss Clyne, A. 2012, Int. J. Mol. Sci., 2012, 13, 5554.
18. Park, K., Lee, S., Kang, E., Kim, K., Choi, K., and Kwon, I.C. 2009, Adv. Funct. Mater., 19,1553.
19. Mérian, J., Gravier, J., Navarro, F., and Texier, I. 2012, Molecules, 17, 5564.
20. Laurent, S., Forge, D., Port, M., Roch, A., Robic, C., Vander Elst, L., and Muller, R.N. 2008, Chem. Rev., 108, 2064.
21. Frascione, D., Diwoky, C., Almer, G., Opriessnig, P., Vonach, C., Gradauer, K., Leitinger, G.., Mangge, H., Stollberger, R., and Prassl, R. 2012, Int. J. Nanomedicine, 7, 2349.
22. Panyam, J., and Labhasetwar, V. 2003, Adv. Drug Deliv. Rev. 55, 329.
23. Kim, J-H., Park, K., Nam, H.Y., Lee, S., Kim, K., and Kwon, I.C. 2007, Prog. Polymer Sci., 32,:1031,
24. Nagavarma, B.V.N., Yadav, H.K.S., Ayaz, A., Vasudha, L.S., and Shivakumar, H.G. 2012, Asian J. Pharm. Clin. Res., 5, 16.
25. Michalet, X., Pinaud, F.F., Bentolila, L.A., Tsay, J.M., Doose, S., Li, J.J., Sundaresan, G., Wu, A.M., Gambhir, S.S., and Weiss, S. 2005, Science, 307, 538.
26. Walling, M.A. 2009, Int. J. of Mol. Sci., 10, 441.
27. Mulder, W.J., Strijkers, G.J., van Tilborg, G.A., Griffioen, A.W., and Nicolay, K. 2006, NMR Biomed., 19, 142.
28. Petersen, A.L., Hansen, A.E., Gabizon, A., and Andresen, T.L. 2012, Adv. Drug Deliv. Rev. 64, 1417.
29. Maeda, H., Wu, J., Sawa, T., Matsumura, Y., and Hori, K. 2000, J. Control. Release, 65, 271.
30. Maeda, H. 2012, J. Control. Release, 164, 138.
31. Saini, S., Stark, D.D., Hahn, P.F., Wittenberg, J., Brady, T.J., and Ferrucci, J.T. Radiology, 162, 211.
32. Simon, G.H., von Vopelius-Feldt, J., Wendland, M.F., Fu, Y., Piontek, G., Schlegel, J., Chen, M.H., and Daldrup-Link, H.E. 2006, J. Magn. Reson. Imaging, 23, 720.
33. Tourdias, T., Roggerone, S., Filippi, M., Kanagaki, M., Rovaris, M., Miller, D.H., Petry, K.G., Brochet, B., Pruvo, J-P., Radüe, E-W., and Dousset, V. 2012, Radiology, 264, 225.
34. Bae, Y. H., and Park, K. 2011, J. Control. Release, 153, 198.
35. Wesselinova, D. 2011, Curr. Cancer Drug Targets, 11, 164.
36. Elbayoumi, T., and Weissig, V. 2009, J. Biomed. Nanotechnol, 5, 620.
37. Yu, M.K., Park, J., and Jon, S. 2012, Theranostics 2, 3.
38. Pirollo, K.F., and Chang, E.H. 2008, Trends in biotechnology, 26, 552.
39. Hadjipanayis, C.G., Machaidze, R., Kaluzova, M., Wang, L., Schuette, A.J., Chen, H., Wu, X., and Mao, H. 2010, Cancer Res. 70, 6303.
40. Lu, R.M., Chang, Y.L., Chen, M.S., and Wu, H.C. 2011, Biomaterials, 32, 3265.
41. Wang, X., Qian, X., Beitler, J.J., Chen, Z., Khuri, F.R., Lewis, M.M., Shin H.J-C., Nie, S., and Shin, D.M. 2011, Cancer Res., 71, 1526.
42. Ross, J.F., Chaudhuri, P.K., and Ratnam, M. 1994, Cancer 73, 2432.
43. Sega, E.I., and Low, P.S. 2008, Cancer Metastasis Reviews, 27, 655.

44. Low, P.S., and Kularatne, S.A. 2009, Curr. Opin. Chem. Biol., 13, 256.
45. Choi, H., Choi, S.R., Zhou, R., Kung, H.F., and Chen, I. 2004, Acad. Radiol., 11, 996.
46. Hong, G.B., Zhou, J.X., and Yuan, R.X. 2012, Int. J. Nanomedicine, 7:2863.
47. Yue, C., Liu, P., Zheng, M., Zhao, P., Wang, Y., Ma, Y., and Cai, L. 2013, Biomaterials, 34, 6853.
48. Kresse, M., Wagner, S., Pfefferer, D., Lawaczeck, R., Elste, V., and Semmler, W. 1998, Magn. Reson. Med., 40, 236.
49. Zhuo, H., Peng, Y., Yao, Q., Zhou, N., Zhou, S., He, J., Fang, Y., Li, X., Jin, H., Lu, X., and Zhao, Y. 2013, Clin. Cancer. Res. Jun 12. [Epub ahead of print]
50. Yang, L., Peng, X.H., Wang, Y.A., Wang, X., Cao, Z., Ni, C., Karna, P., Zhang, X., Wood, W.C., Gao, X., Nie, S., and Mao, H. 2009, Clin. Cancer Res. 15, 4722.
51. Wang, L,.Su, W., Liu, Z., Zhou, M., Chen, S., Chen, Y., Lu, D., Liu, Y., Fan, Y., Zheng, Y., Han, Z., Kong, D., Wu, J.C., Xiang, R., and Li, Z. 2012, Biomaterials, 33, 5107.
52. Desgrosellier, J.S., and Cheresh, D.A. 2010, Nat. Rev. Cancer, 10, 9.
53. Danhier F., Le Breton, A., and Préat, V. 2012, Mol. Pharm. 9, 2961.
54. Cai, W., Shin, D.W., Chen, K., Gheysens, O., Cao, Q.Z., Wang, S.X., Gambhir, S.S., and Chen, X. 2006, Nano Lett., 6, 669.
55. Murphy, E.A., Majeti, B.K., Barnes, L.A., Makale, M., Weis, S.M., Lutu-Fuga, K., Wrasidlo, W., and Cheresh, D.A. 2008, Proc. Natl. Acad. Sci. USA, 105, 9343.
56. Chacko, A.M., Hood, E.D., Zern, B.J., and Muzykantov, V.R. 2011, Curr. Opin. Colloid Interface Sci. 16, 215.
57. Hamilton, A.J., Huang, S.L., Warnick, D., Rabbat, M., Kane, B., Nagaraj, A., Klegerman, M., and McPherson, D.D. 2004, J. Am. Coll. Cardiol. 43, 453.
58. Tsourkas, A., Shinde-Patil, V.R., Patel, Kelly, K.A., Patel, P., Wolley, A., Allport, J.R., and Weissleder, R. 2005, Bioconjug. Chem., 16, 576.
59. Nahrendorf, M., Jaffer, F.A., Kelly, K.A., Sosnovik, D.E., Aikawa, E., Libby, P., and Weissleder, R. 2006, Circulation, 114, 1504.
60. Southworth, R., Kaneda, M., Chen, J., Zhang, L., Zhang, H., Yang, X., Razavi, R., Lanza, G., and Wickline, S.A. 2009, Nanomedicine 5, 359.
61. McAteer MA, Sibson NR, von Zur Muhlen C, Schneider JE, Lowe AS, Warrick N Channon KM, Anthony DC, Choudhury RP. In vivo magnetic resonance imaging of acute brain inflammation using microparticles of iron oxide. Nature Medicine 13, 1253 - 1258 (2007)
62. Reynolds, P.R., Larkman, D.J., Haskard, D.O., Hajnal, J.V., Kennea, N.L., George, A.J., and Edwards, A.D. 2006, Radiology 241, 469.
63. Chapon, C., Franconi, F., Lacoeuille, F., Hindre, F., Saulnier, P., Benoit, J.P., Le Jeune, J.J., and Lemaire, L. 2009, Magma 22, 167.
64. van Kasteren, S.I., Campbell, S.J., Serres, S., Anthony, D.C., Sibson, N.R., and Davis, B.G. 2009, Proc. Natl. Acad. Sci. U S A 106, 18.
65. Jin, A.Y., Tuor, U.I., Rushforth, D., Filfil, R., Kaur, J., Ni, F., Tomanek, B., and Barber, P.A. 2009, Contrast Media Mol. Imaging 4, 305.
66. Suzuki, M., Serfaty, J.M., Bachelet, L., Beilvert, A., Louedec, L., Chaubet, F., Michel, J.B., and Letourneur, D. 2011, J. Cardiovasc. Magn. Reson. 13, Suppl 1, P372.

67. Stevenson, R., Axel, J., Hueber, A.J. Hutton, A., McInnes, I.B., and Graham, D. 2011, Scientific World Journal, 11, 1300.
68. Moore, A., Grimm, J., Han, B., and Santamaria, P. 2004, Diabetes, 53, 1459.
69. Majmudar, M.D., Yoo, J., Keliher, E.J., Truelove, J.J., Iwamoto, Y., Sena, B., Dutta, P., Borodovsky, A., Fitzgerald, K., Di Carli, M.F., Libby, P., Anderson, D.G., Swirski, F.K., Weissleder, R., and Nahrendorf, M. 2013, Circ. Res., 112, 755.
70. Utsugi, T., Schroit, A.J., Connor, J., Bucana, C.D., and Fidler, I.J. 1991, Cancer Res., 51, 3062.
71. Ran, S., Downes, A., and Thorpe, P.E. 2002, Cancer Res., 62, 6132.
72. Ran, S., and Thorpe, P.E. 2002, Int. J. Radiat. Oncol. Biol. Phys., 54, 1479.
73. Huynh, M.L., Fadok, V.A., and Henson, P.M. 2002, J. Clin. Invest., 109, 41.
74. Serhan, C.N., Brain, S.D., Buckley, C.D., Gilroy, D.W., Haslett, C., O'Neill, L.A.J., Perretti, M., Rossi, A.G., and Wallace. J.L. 2007, FASEB J., 21, 325.
75. Blankenberg, F.G., and Strauss, H.W. 2012, J. Nucl. Med., 53, 1659.
76. Blankenberg, F.G., and Strauss, H.W. 2013, J. Nucl. Med., 54, 1.
77. Belhocine, T., Steinmetz, N., Green, A., and Rigo, P. 2003, Ann. N.Y. Acad. Sci., 1010, 525.
78. Niu, G., and Chen, X. 2012, J. Nucl. Med., 51, 1659.
79. Prinzen, L., Miserus, R.J.J.H.M., Dirksen, A., Hackeng, T.M., Deckers, N., Bitsch, N.J., Megens, R.T.A., Douma, K., Heemskerk, J.W., Kooi, M.E., Frederik, P.M., Slaaf, D.W., van Zandvoort, M.A.M.J., and Reutelingsperger, C.P.M. 2007, Nano Lett., 7, 93.
80. van Tilborg, G.A.F., Vucic, E., Strijkers, G.J., Cormode, D.P., Mani, V., Skajaa, T., Reutelingsperger, C.P.M., Fayad, Z.A., Mulder, W.J.M., and Nicolay, K. 2010, Bioconjug. Chem., 21, 1794.
81. Zhang, R., Huang, M., Zhou, M., Wen, X., Huang, Q., and Li, C. 2013, Mol. Imaging, 12, 182.
82. Vaccaro, A.M., Tatti, M., Ciaffoni, F., Salvioli, R., Serafino, A., and Barca, A. 1994, FEBS Lett., 349, 181.
83. Qi, X., and Chu, Z. 2004, Arch. Biochem. Biophys. 424, 210.
84. Qi, X., Chu, Z., Mahller, Y.Y., Stringer, K.F., Witte, D.P., and Cripe, T.P. 2009, Clin. Cancer Res., 15, 5840.
85. Abu-Baker, S., Chu, Z., Stevens, A.M., Li, J., and Qi, X. (2012). J. Cancer Ther., 3, 321.
86. Wojton, J., Chu, Z., Mathsyaraja, H., Meisen, W.H., Denton, N., Kwon, C.H., Chow, L.M., Palascak, M., Franco, R., Bourdeau, T., Thornton, S., Ostrowski, M.C., Kaur, B., and Qi, X. 2013, Mol. Ther. Jun 4. [Epub ahead of print]
87. Bogdanov, A.A. Jr., Martin, C., Weissleder, R., and Brady, T.J. 1994, Biochim. Biophys. Acta, 1193, 212.
88. Kaimal, V., Chu, Z., Mahller, Y.Y., Papahadjopoulos-Sternberg, B., Cripe, T.P., Holland, S.K., and Qi, X. 2011. Mol. Imaging Biol., 13, 886.
89. He, X., Wang, K., and Cheng, Z. 2010, Wiley Interdiscip. Rev. Nanomed. Nanobiotechnol., 2, 349.
90. Qi, X, Flick, M.J., Frederick, M., Chu, Z., Mason, R., DeLay, M., and Thornton, S. 2012, PLoS ONE, 7, 1.